Environ Geochem Health (2024) 46:239
https://doi.org/10.1007/s10653-024-01971-y

ORIGINAL PAPER

The chemical state of the watershed in Ras Elma region (South of Taza, Morocco) one of the parameters responsible for the decline in the formation of the current travertine formations

Kamal Lahrichi · Jaouad Gartet · Marouane Laaraj · Jamal Naoura · Hamid Fattasse · Abdelmonaim Okacha

Received: 22 January 2024 / Accepted: 26 March 2024 / Published online: 7 June 2024

Abstract The Ras Elma region, situated to the south of the city of Taza in northern Morocco, boasts abundant travertine formations that continue to develop, albeit selectively in specific sheltered sites. This development is influenced by various parameters, including the role of water chemistry. This article presents a spatio-temporal analysis of various hydrochemical parameters, including conductivity, pH, temperature, magnesium, calcium, and others. It's worth noting that the water from the Ras Elma Vauclusian spring, a key driver of travertinization in the region, is sourced from water infiltrating through faults and flowing into Lake Tompraire, known as Dayat Chikker near the Bab Boudir area. The findings suggest that the water in Ras Elma has turned aggressive, as revealed by the examination of the calcaro-carbonic equilibrium. $CaCO_3$ precipitation occurs predominantly in the summer, significantly impacting the formation of travertines, particularly those of the spring and dam types. However, valley-type travertines exhibit more extensive development compared to the other two types.

Keywords Ras Elma · Water · Travertine · Hydrochemistry · Precipitation

K. Lahrichi · J. Gartet · H. Fattasse
Laboratory EH3D, University of Sidi Mohammed Ben Abdellah, Route d'Imouzzer, P.O. Box 2202, 30 000 Fez, Morocco
e-mail: lahrichi.kamal@gmail.com

M. Laaraj (✉)
Laboratory of Functional Ecology and Environment Engineering, University of Sidi Mohammed Ben Abdellah, Route d'Imouzzer, P.O. Box 2202, 30 000 Fez, Morocco
e-mail: marouane.laaraj@usmba.ac.ma

J. Naoura
Laboratory of Natural Resources and Environment, University of Sidi Mohammed Ben Abdellah, Route d'Imouzzer, P.O. Box 2202, 30 000 Fez, Morocco

A. Okacha
Geography and Development Group, FLSH, Abdelmalek Esaadi University, Martil, Morocco

Introduction

Travertine, a sedimentary rock of continental limestone, is identified by its density, finely crystalline structure, compactness, or mass, often presenting a concretionary appearance with fluctuating levels of vacuolization. Its color varies from gray to yellowish, and it commonly features coarse layering formed through the swift precipitation of calcium carbonate as a result of water agitation or evaporation (Foucault & Raoult, 1980). These formations are found across the globe (Chafetz & Folk, 1984; Luo et al., 2022).

Travertine and/or tufa possess both ecological and technical significance, serving as effective mediums for water storage and drainage due to their loose and porous structure. These formations, known for their vibrant colors and clear water, have become

popular tourist destinations (Yan et al., 2023). The term refers to non-marine carbonate sediments situated near sources, rivers, lakes, and caves, predominantly composed of calcite (Akin & Özsan, 2011; Pentecost, 2005). Travertine can be categorized into two types: the precipitation of calcium carbonate at room temperature in cold water and the deposition of calcium carbonate near hot springs (Ford & Pedley, 1996). A comprehensive understanding of travertine formation is essential for elucidating the local hydrological cycle's migration process. Consequently, the stratified and zonal structure resulting from periodic sedimentation imparts scientific value, particularly in terms of paleoclimate and paleohydrogeology, notably in the Quaternary (Liu et al., 2015). According to the relief and sedimentary environment, the main types of travertine deposits can be classified into the following forms (Asta et al., 1977; Cook & Chafetz, 2017): pool, beach flow, lake, karstic cave, and waterfall, ranging from horizontal to nearly vertical. Morphological changes in travertine sediments may result from various deposition patterns, distinct mineral compositions, and different flow directions (Claes et al., 2017; Kalender et al., 2015), while erosion can alter their morphology (Fouke et al., 2000). The minerals constituting these various types of travertine provide sensitive environmental records of hydrochemistry, hydrological transmission, and climate (Bonny & Jones, 2008), thus facilitating paleoenvironmental reconstruction. For instance, barite deposition in travertine is influenced by the oxidation state of spring water, the rate of carbon dioxide degassing, and microorganisms (Pentecost, 1995). The predominant minerals in travertine deposits are calcite and aragonite (Özkul et al., 2013). Additionally, isotopic data in tufa can offer valuable insights into the study of climate and temperature (Andrews, 2006; Quade et al., 2017). In travertine formed during different seasons, the values of stable carbon and oxygen isotopes vary (Kele et al., 2008) and gradually increase from spring to the end of the system (Drysdale et al., 2002).

Several researchers have also explored travertine (Zhao et al., 2022), demonstrating the interdependence among slope, basin, and waterfall travertine deposits in the Huanglong basin. Ismail and Ahmed (2023) and Ehya and Marbouti (2018) have examined changes in hydrochemistry downstream along the flow path and the influence of hydrodynamics on CO_2 degassing and $CaCO_3$ precipitation. Zhang et al., (2012) predicted the rate of $CaCO_3$ precipitation resulting from hydrochemistry in rapidly moving water. However, these studies did not thoroughly investigate the role of other potential factors in controlling travertine deposition. Furthermore, with the increase in tourist activities, much remains to be done for the preservation of travertine.

Ras Elma, located in the Tazekka National Park in Morocco, is renowned for its abundant travertine deposit, presumably formed during the Holocene. Three main categories of travertines emerge here, classified based on the valley morphology extending from the source of Ras Elma to the Oued Taza Valley: source, barrage, and valley, a classification inspired by the works of (Bakalowicz, 1990; Casanova, 1981). However, the current formation of travertines is declining, impacted by various factors such as climate, human intervention, and alterations in water chemistry. As a result, the regional travertine system has been disrupted, primarily by the crushing and destruction of ancient travertine terraces.

Furthermore, the water of Ras Elma has become more aggressive, exhibiting undersaturation in dissolved calcium carbonate ($CaCO_3$), as evidenced by the Ryznar and Langelier methods. The assessment of potential calcium carbonate precipitation (PCCP) highlights significant precipitation, especially in July, August, September, and October, in the central area of Ras Elma, where source and barrage-type travertins form. Conversely, the formation of valley-type travertins is influenced by the waters of Oued El Heddar, characterized by calcium carbonate oversaturation, with a considerable PCCP throughout the year.

This study is particularly significant for two primary reasons. Firstly, it represents the inaugural effort to reveal the hydrochemical characteristics of the Ras Elma World Heritage site. Secondly, it enhances our comprehension of the current h^{2}ydrochemical process associated with travertine deposition, offering valuable insights for preserving travertine and interpreting the sedimentary environment.

Geographical location of the study sites

The area under investigation in our study is situated to the south of the Taza region in northeastern Morocco (Fig. 1), thereby forming a sub-basin within the upper reaches of the extensive Sebou basin. This particular zone encompasses the juncture between the folded Middle Atlas and the marly tertiary rocks. Rainwater descends upon the perimeters of Lake Tompraire of Chikker, subsequently seeping through absorption points (such as dolines, ponors, and avens). Following a path into the depths, this water resurfaces at the Ras Elma spring, constituting one of the water sources for the Oued El Heddar (a sub-tributary of the Oued Taza).

A hydrochemical study of the water was conducted at two sites: Ras Elma upstream and Oued El heddar downstream. The aim was to ascertain the variability of geochemical parameters including conductivity, turbidity, dissolved oxygen, Mg^{2+}, Ca^{2+}, and HCO_3^-. These factors contribute to the formation of the present travertines at both locations.

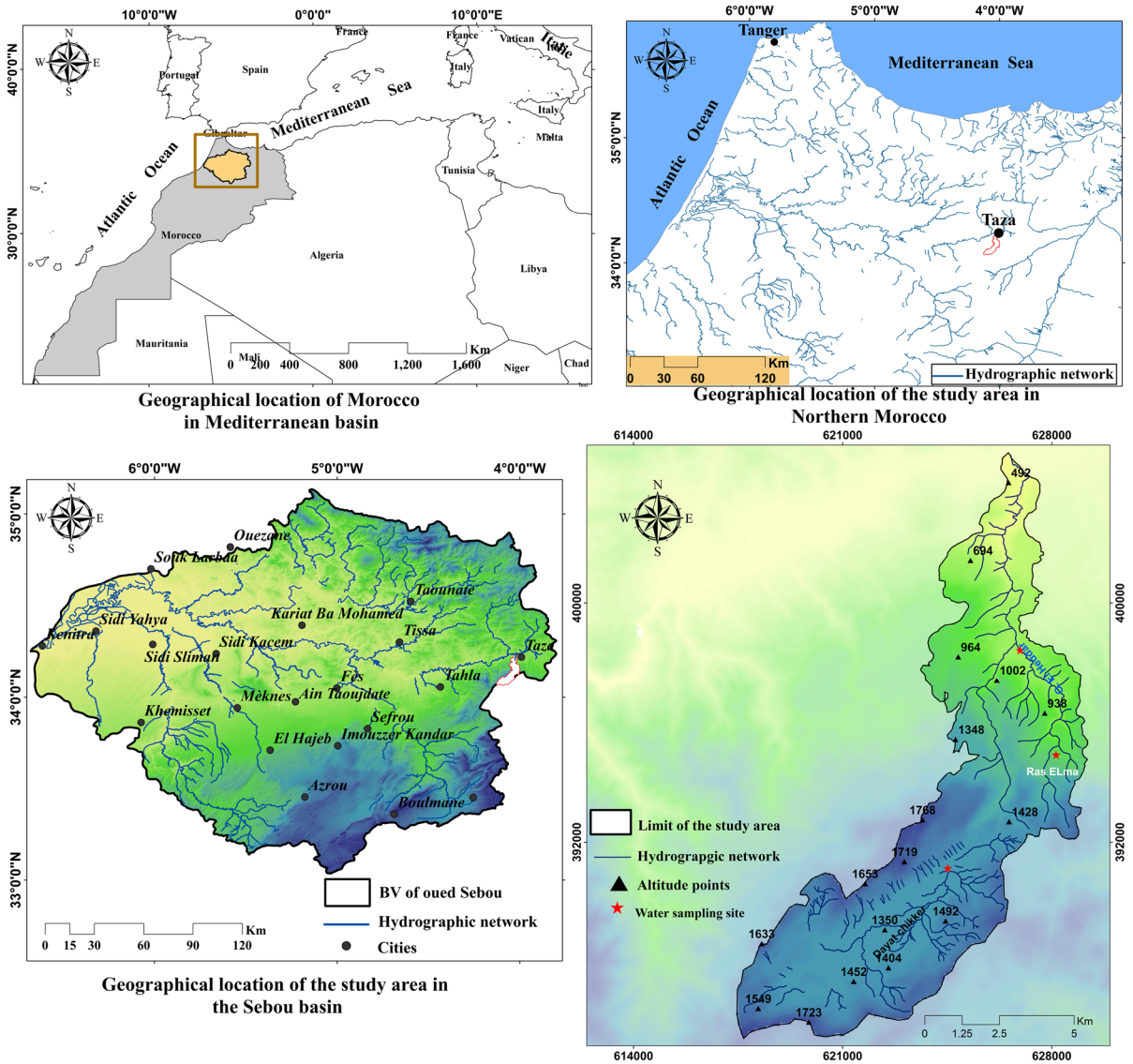

Fig. 1 Geographical location of the Ras Elma hydrogeological watershed

The climatic context

Climate stands as one of the primary influencers in travertine formation. The sedimentation mechanisms align particularly well with climatic conditions characterized by moderate temperatures and specific patterns of precipitation distribution and intensity. These conditions facilitate various factors, notably the proliferation of vegetation and soil cover rich in CO_2, alongside abundant and consistent freshwater runoff (Weisrock et al., 1986).

The climatic analysis offers insights into the origin of Ras Elma spring water, which has been the pivotal force driving current travertine formation in our study area. Multiple studies suggest that the spring water results from the infiltration of water from Dayat Chikker through zones of vulnerability such as faults and ponors, ultimately emerging at Ras Elma.

The study area, situated between the Middle Atlas in the south and the Pri-Rif in the north, falls within the context of the Mediterranean climate. The climate here spans from semi-arid to sub-humid and humid, maintaining a predominantly continental nature. The presence of chergui winds significantly impacts higher temperatures. In essence, our study area and its environs are delineated by their precipitation levels, specifically in terms of the frequency of rainy days. This frequency fluctuates across different rainfall stations owing to various factors, notably orography and the orientation of slopes.

To investigate the climate, we utilized data from two rainfall stations: the Bab Boudir station near Dayat Chikker upstream and the Taza station downstream. The Annual rainfall at the two stations ranges from 1976 to 2017, with an annual maximum recorded in 2010 at 850 mm and an annual minimum recorded in 1995 at 230mm at the Taza station. However, the Bab Boudir station recorded an annual maximum of 2000 mm in 1996 and a minimum of 310 mm in 2012. The variation in annual rainfall rates between the two stations can be explained by a number of factors, including the altitude factor and the geographical location of Bab Boudir. Indeed, the high relief of Bab Boudir acts as an embankment against the humid air masses that come from the west of Morocco, and consequently the rainfall rate increases.

Temperature indirectly influences travertine formation. Rainwater, nearly devoid of cations and minimally mineralized, contains CO_2 in equilibrium with the atmosphere and maintains an acidic nature. When this equilibrium water, at 5 to 15°C, warms, it loses 25% of its dissolved CO_2, precipitating 25% of its dissolved calcite (Thiry & Jean, 2013). The lowest recorded temperature at Bab Boudir in January was − 2.8°C, whereas the highest in July was 29.3°C. Contrastingly, Taza experienced a minimum of 5.8°C and a maximum of 35.1°C.

This climatic pattern ensures a consistent water supply to the Ras Elma spring, with monthly flows fluctuating between a peak monthly average of approximately 500 l/s in February and a minimum monthly average of around 46 l/s in August and 49 l/s in September.

Lithology of the study area

The lithological composition of the massif stands as one of the pivotal elements influencing travertinisation. Specifically, the precipitation and formation of limestone tuffs and travertines require the presence of an upstream region abundant in highly porous carbonate rocks like sandstone, limestone, and dolomite. These rocks often feature extensive submerged areas where the solution accumulates a significant portion of its mineral content, typically attaining saturation (Nicod, 1986).

In a general sense, the outcrops within our study area exhibit a diverse range of ages and lithological compositions. The Mesozoic outcrops notably feature a prevalence of limestone-dolomitic rocks, whereas the Cenozoic outcrops situated in the north are distinguished by soft Miocene formations (Hoepffner, 1978).

As per the geological map, the Triassic formations overlay the Paleozoic substrata in a non-conformable manner. These formations are of the coarse detrital type and exhibit saliferous clay outcrops along the significant tectonic faults within the Middle Atlas (Sabaoui & Viallard, 1987).

The outcrops of the lower Lias (Sinemurian) manifest as dolomitic limestone and marl at their base, overlaying the Triassic formations, as outlined in the study by (Robillard, 1981). This study provides the following description: "These carbonate formations consistently rest atop the basal Triassic-Lias." Moving into the Domerian stage, the outcrops expand slightly, forming sequences of limestone banks interspersed with marl layers. By the Toarcian stage,

there's a discernible shift in the facies of the marly limestone rocks that overlie the Domerian formations.

The northern section is characterized by an abundance of soft rocks from the Tertiary period, exhibiting a structure of blues marl occasionally intermixed with sand, as precisely depicted by (Gentil, 1911) during the Tortonian–Messinian period.

Within the study area, the Quaternary era is identified by travertine deposits, accumulations of scree, fluvial sediments, and decalcification soil deposits (Fig. 2).

Tufa and travertine formations in the Ras Elma region:

The Ras Elma region exhibits a diverse array of travertine forms and formations, ranging from ancient to actively forming structures. These encompass three primary categories, as previously delineated by Casanova in 1981. The spring-type travertines within this category notably bear the trace of human settlement, marked by the construction of residences and infrastructure dating from the colonial era to the present day. Despite

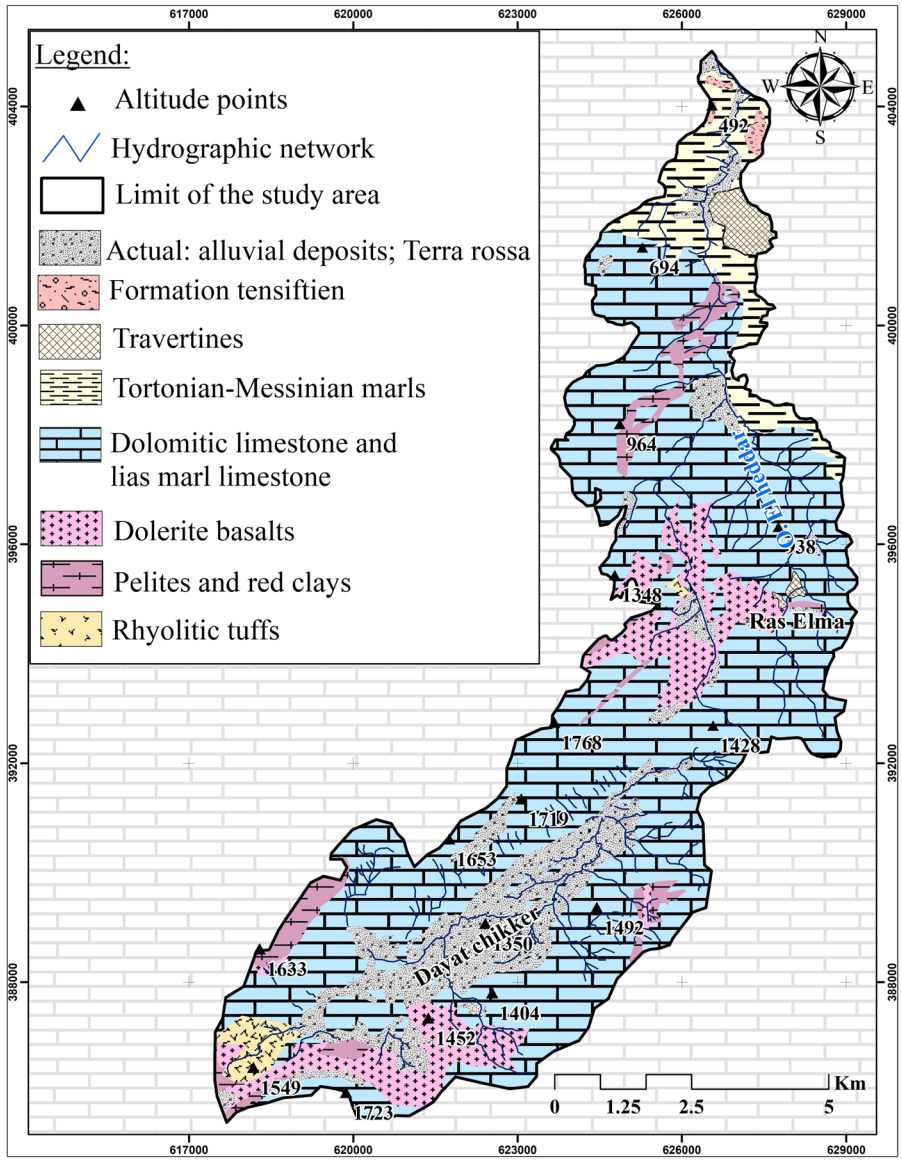

Fig. 2 Lithological context of the study area. (Based on the Taza 1/50000 geological map)

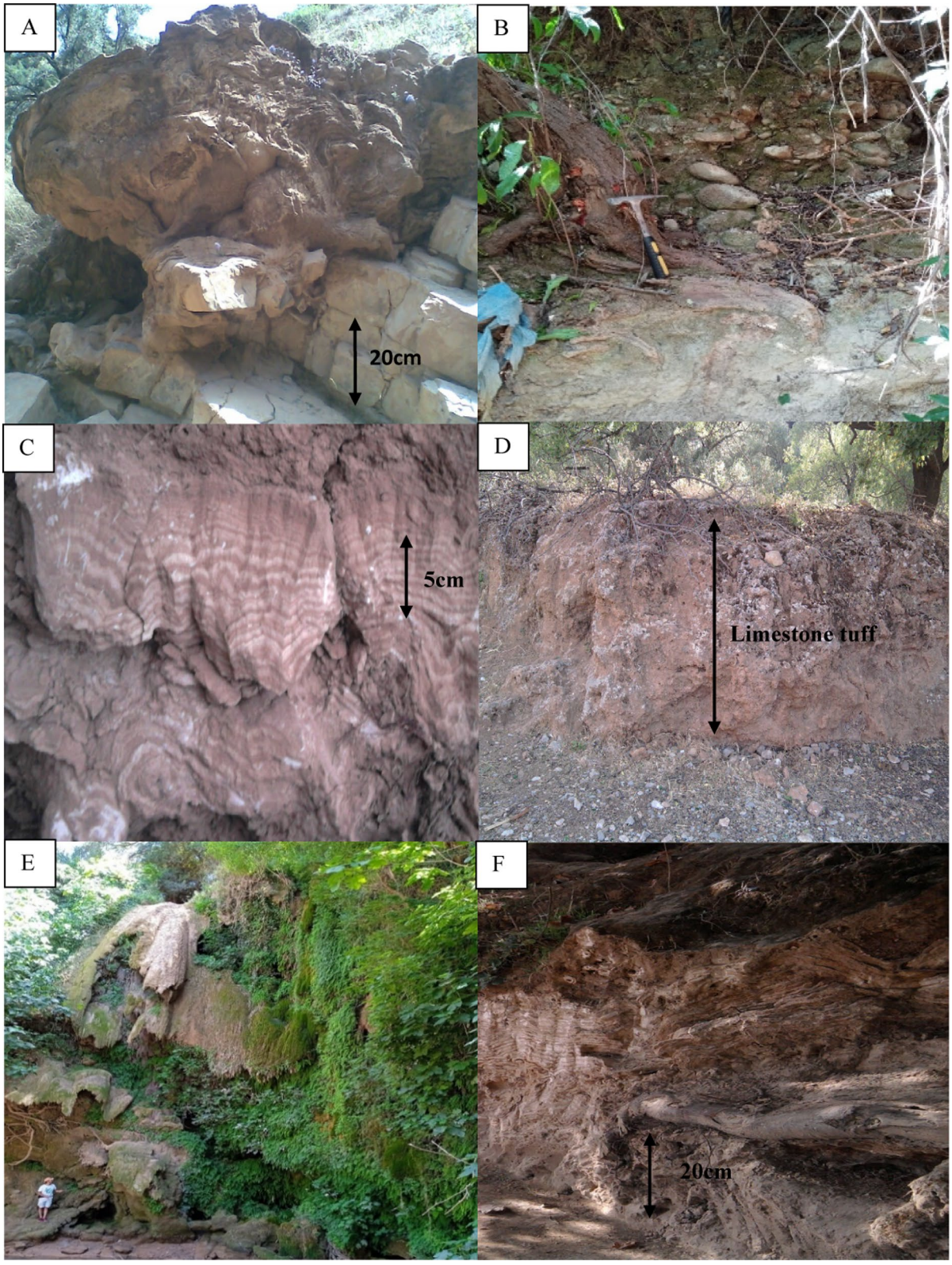
A
20cm
B
C
5cm
D
Limestone tuff
E
F
20cm

◂**Fig. 3** Geomorphological aspects of the travertines in the Ras Elma region **a** travertine deposited directly on marl-limestone **b** valley-type travertine **c** Laminated travertine **d** Limestone tuff E-the great waterfall of the ras Elma region F-travertine formed on tree trunks.

this, within the channel formed by the spring, one encounters pebbles encrusted by the precipitation of calcium carbonates. Moving beyond the initial waterfall, situated approximately 200m from the source, lies the second category: the travertines of the dam type. Within this segment, there exist three major generational phases from the initial waterfall to the expansive cascade situated within the study area. This succession delineates a series of water reservoirs and waterfalls, their formation contingent upon the morphology of the Oued El Heddar watercourse. Furthermore, in select areas, the construction of travertine dam's results from the presence of substantial blocks or clusters of vegetation (Mounir et al., 2019).

The extensive 15-m cascade (Fig. 3; Photo A) at Ras Elma is formed by lengthy draperies of bryophytes, specifically mosses, created during serene, continuous streams. Beneath these formations lie small caves or shelters formed due to the advancement of these draperies. Below this cascade, crusts appear on blocks resulting from the lateral collapse of dolomitic limestone rocks, as well as on various plant supports such as stems, branches, and roots. Additionally, the Ras Elma area is characterized by the presence of laminated travertines (Adolphe, 1981; Casanova, 1981; Vaudour, 1986). This type of travertine often encapsulates numerous plant remnants such as leaves, trunks, and mosses, among others, with its morphology contingent upon the substrate it develops upon. These formations are typically associated with highly dynamic hydrological environments.

This facies presents a distinguishable succession, visible to the naked eye on a macroscopic scale, featuring alternating light and dark laminae. This alternation takes the form of laminae exhibiting microsparitic to sparitic precipitation (light laminae) alongside laminae demonstrating micritic precipitation (dark laminae).

The valley-type travertines develop post the aforementioned large cascade, extending over 4km from the Ras Elma source to the Oued Banon confluence with the Oued El Heddar. Within this stretch, various facies have emerged, predominantly featuring travertino-detritic type formations, travertines supported by plants, and laminated stromatholitic travertines.

Figure 3 (photo A) illustrates a valley-type travertine structure observed after the aforementioned significant waterfall. It manifests as centimeter-thick laminae composed of stromatholitic algal mats. Conversely, photo (B) displays a detritic travertine facies at the base, covered by alluvium comprising pebbles and more or less rounded gravels.

Another prevalent travertine facies, resembling tree trunks, is widely dispersed along the Oued El Heddar, owing to the dense presence of trees along its banks. During winter, the Oued El Heddar's water flow intensifies, leading to the uprooting of trees along its path. In other seasons, the water flow subsides and becomes rich in calcium bicarbonate. Upon encountering a tree trunk, the water mineralizes it, effectively transforming it into a small dam (photo F). The Fig. 3 photo (D) depicts a section of calcareous tuff situated within a small tectonic depression bounded by geographical coordinates (34°09′09′′N; 4°00′49′′W). This section, over 1m thick and dark brown in color, comprises a blend of fine and coarse sands, along with carbonate elements. It is topped by hydrophilic plant remains and continental plant residues, formed during the recent Pleistocene period.

Materials and methods

The Ras Elma site has been the focal point of numerous research excursions aimed at mapping the distribution of tufa and travertine, understanding their topographic and sedimentological positioning, and conducting a lithofacies study. Regarding hydrochemical analysis, 12 water samples were collected in sterile containers as grab samples, following the general protocol for sample storage and handling (ISO, 1994), at three sites (Dayat Chikker, Ras Elma, and Oued El Heddar) on a monthly basis between January 2021 and December 2021.

The study focused on a set of physicochemical parameters. On-site measurements included temperature, pH, and electrical conductivity, assessed using a CONSORT-Model835 multiparameter analyzer. Turbidity was measured with a portable turbidimeter compliant with ISO—HI98713, and dissolved oxygen was determined using Hanna Instruments ISO- HI9142

equipment. Various reagents, including hydrochloric acid (HCl^-), EDTA solution, sodium hydroxide (NaOH), ammonia solution (NH_3OH), silver nitrate ($AgNO_3$), and potassium chromate (K_2CrO), were used for the determination of cations (Ca^{2+}, Mg^{2+}, Na^+, K^+) and anions (HCO_3^-, Cl^-, SO_4^{2-}) in the sampled water, following the Rodier et al. (2009) protocol. All these analyses were conducted at the RADDETA laboratory (Autonomous Water and Electricity Distribution Authority) in Taza.

The PHREEQC geochemical program (Plummer, 1984) was used to identify the main hydrogeochemical facies of the studied sites and to calculate the saturation index of minerals such as anhydrite, aragonite, calcite, dolomite, gypsum, and halite.

In the context of an in-depth study, this article assesses the ability of carbonate rocks to dissolve and precipitate $CaCO_3$ in the Ras Elma region. The Langelier and Ryznar indices are employed to evaluate the capacity of carbonate rocks to dissolve and precipitate $CaCO_3$ in a given water system. These indices take into account specific physico-chemical parameters such as water temperature, pH, conductivity, Ca^{2+} content, and bicarbonates (HCO_3^-) (Srour et al., 2022). The Langelier Saturation Index (LSI) measures the saturation of calcium carbonate in water, while the Ryznar Stability Index (RSI) is used to predict the likelihood of calcium carbonate scaling. Both indices are crucial for understanding the potential dissolution and precipitation of minerals in water systems, especially in connection with carbonate rocks (Santhanam et al., 2021). The use of these indices is well-documented in the literature and is commonly employed in geochemical modeling and water quality assessments (Ghobadi Nia et al., 2010; Palazzo et al., 2015).

Results

Principal hydrogeochemical facies

The Piper diagram illustrates cations and anions on two distinct triangles, each side displaying the proportion of major ions concerning the total ions. The position of an analysis on these triangles helps ascertain dominance in both cations and anions. These triangles are linked to form a rhombus, marking the convergence of lines drawn from the identified points on each triangle. This convergence point represents the comprehensive analysis of the sample, aiding in specifying the water's facies.

Analysis of the Piper diagram reveals that samples grouped under (A) exhibit a calcic to magnesian facies across the three studied sites. The area denoted by the letter (B), representing cations, displays a calcic to magnesian bicarbonate composition, comprising 50% (Ca^{2+}) and 50% (Mg^{2+}) across these sites. In contrast, the zone marked by the letter (C), representing anions, signifies bicarbonated water. Overall, the diagram depicts a water family predominantly characterized by calcium and magnesium bicarbonate compositions (Fig. 4).

The various facies unveil the hydrogeochemical processes governing groundwater mineralization across the three studied sites. This examination hinges primarily on the outcomes of chemical analyses conducted. These findings showcase minimal content variance, with most cases indicating standard deviations below the mean (Table 1).

Given that standard deviation measures the spread of values around the mean, the smaller standard deviation values in this instance suggest reduced dispersion among the variables.

From the results provided in the same table, it's evident that the studied waters exhibit an average temperature of 13.12 °C, notably higher this year

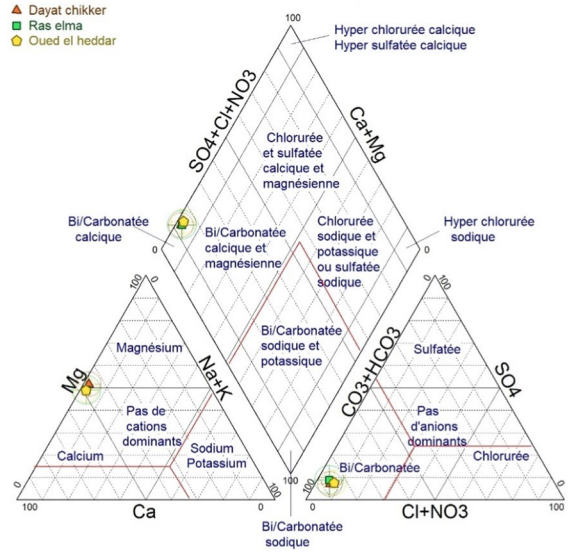

Fig. 4 Graphical representation of chemical facies Piper diagram (dayat Chikker, Ras Elma and Oued El Heddar)

(attributed to the persistent drought impacting our country in recent years). The waters maintain an average slightly acidic to neutral pH of 6.78. Additionally, their conductivity (µS/cm) indicates high to markedly high mineralization, varying with the seasons. The distribution of cations and anions in the studied waters follows this order: Ca^{2+}, Mg^{2+}, Na^{+}, K^{+}; HCO_3^{-}, SO_4^{-}, Cl^{-}.

Characteristic ratios

The interrelationships among the chemical elements detected in groundwater Na^{+}, Cl^{-}, SO_4^{2-}, Ca^{2+}, and HCO_3^{-} highlight the prevalence of carbonate ions (Ca^{2+}, HCO_3^{-}) over other ions like saliferous ions (Na^{+}, Cl^{-}). To expound upon these chemical element relationships, we've developed several graphs depicting the ensuing characteristic relationships: The rMg^{2+}/rCa^{2+} ratio.

Table 1 Preliminary results of physicochemical parameters

Variables	Water of the study sites			
	Minimum	Maximum	Average	Standard deviation
T°C	9	24	13.12	4.39
pH	6.85	7.88	6.78	1.22
Cond µS/cm	402	680	502.19	125.74
Turbi	1.6	33.9	9.75	7.96
O_2. dissolved	4.32	8.99	5.37	1.35
Cl^{-}	7.1	15.97	10.76	2.80
Ca^{2+}	84.8	136	93.14	23.85
Mg^{2+}	46	82.5	58.91	15.50
HCO_3^{-}	244	390.4	279.40	70.03
K^{+}	1	8	2.44	2.23
Na^{+}	0.7	8	3.78	2.59
SO_4^{-2}	10	46	20.15	8.67

The rMg^{2+}/rCa^{2+} ratio values (Fig. 5) across the three sites spanned from 0.53 (Oued El Heddar site) to 0.99 (Dayat Chikker site), averaging at 0.64. These values indicate that the rMg^{2+}/rCa^{2+} ratio remained below 1 across all three sites during this measurement year. This signifies calcium's prevalence resulting from the dissolution of carbonate formations within the study area.

The results from the characteristic ratio of rMg^{2+}/rCa^{2+} indicate that all the sites had values lower than 1, signifying the prevalence of calcium. This is attributed to the solubility of calcium-rich limestones rather than magnesium-rich ones (Teboul et al., 2016).

The ratio between $(Na^{+}+k^{+})/Cl^{-}$

The dominance of chlorides is corroborated by the characteristic ratio $(Na^{+}+K^{+})/rCl^{-}$, which remains below 1 at all three sites (Fig. 6), except for the Ras Elma site that records values exceeding 1 in months 8, 11, and 12 of 2021. This is likely a result of water circulation within marl and clay soils.

When the ratio r $(Na^{+}+K^{+})$ $/rCl^{-}$ is less than 1, it indicates a predominance of chlorides, linked to saline soils. When this ratio exceeds 1, sodium prevails.

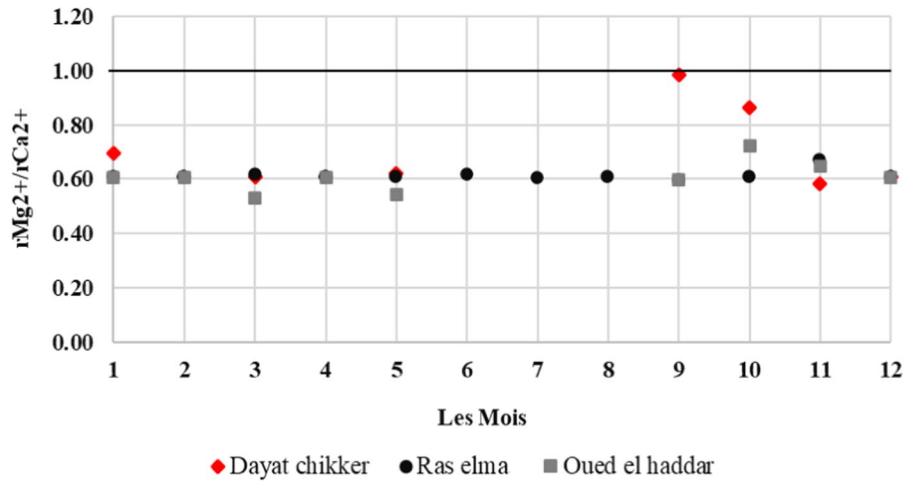

Fig. 5 Characteristic ratio ($rMg^{2+}/rCa.^{2+}$)

Ratio between (SO_4^{2-}/Cl^-)

The characteristic ratio is greater than 1 for the majority of the three sites during the 2021 period. This is explained by an increase in sulphate concentration. However, Oued El Heddar and the Chikker site recorded values below 1 in the months of June, September, and October, reflecting the predominance of chlorides.

The Fig. 7 above illustrates that, throughout the year 2021, all three sites recorded values exceeding 1, with the exception of the month of mai 5 at the Oued El Heddar site that recorded a value of 0.7, and months of September and October at the Dayat Chikker site, that registered 0.9. This scenario indicates a prevalence of sulfates, primarily associated with leaching from gypsum soils and the oxidation of sulfides, notably pyrite. This process occurs when these minerals react with atmospheric oxygen and water, resulting in the formation of sulfuric acid (H_2SO_4) and sulfate ions (SO_4^{2-}). The oxidation of sulfides can be influenced by various factors such as the presence of oxygen, water, microorganisms, and chemical catalysts (Rimstidt & Vaughan, 2003). Furthermore, in investigating the water's nature, particular attention is directed toward the Vaucluse spring of Ras Elma and Oued El Heddar, where ongoing tuff and travertine formations occur. We've employed three methods for this inquiry: the Ryznar method, assessing water tendencies toward aggressiveness or calcium carbonate deposits; the Langelier method, determining whether the water in Ras Elma and Oued El Heddar is saturated or

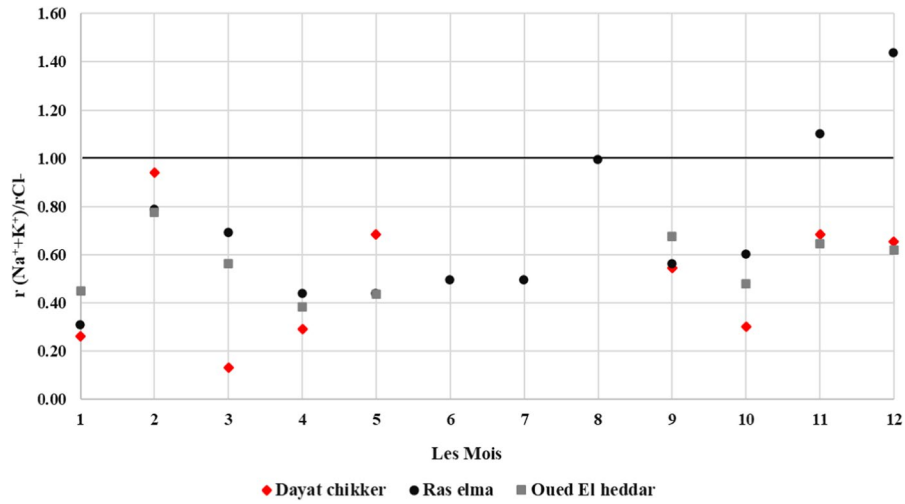

Fig. 6 Characteristic ratio r $(Na^+ + K^+)/rCl^-$

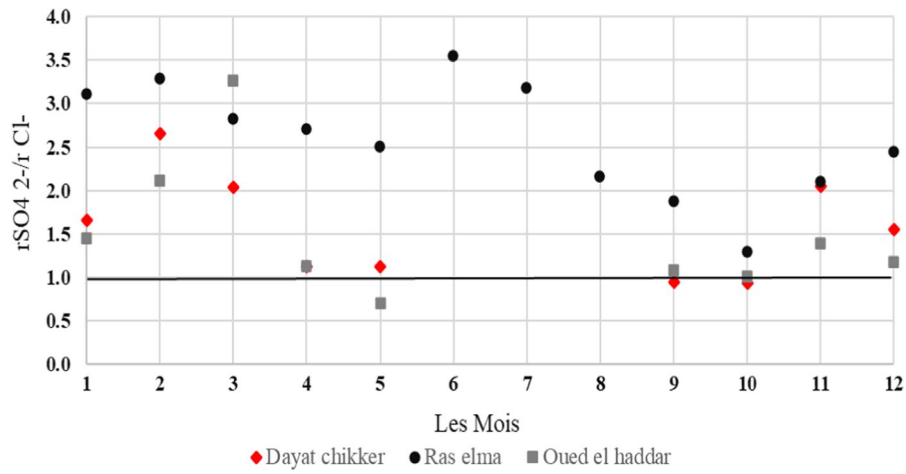

Fig. 7 Characteristic ratio (rSO_4^{2-}/r Cl.$^-$)

undersaturated with calcite, based on the 2021 measurements; and the Hallopeau–Dubin method, theoretically predicting the rate of precipitated calcium carbonate during the measurement year's days. These methods find widespread use among various researchers (Al-Qurnawi et al., 2022; Amouei et al., 2017; Yekta et al., 2015).

The Langelier and Ryznar indices

The Ryznar method is used as an empirical approach to predict the water's nature by assessing its tendency to be corrosive or to deposit calcium carbonate. It is computed using the formula:

$$\mathrm{Ir} = 2\,\mathrm{pHs} - \mathrm{pH}.$$

The saturation pH (pHs), an essential factor, is calculated employing the empirical formula below:

$$\mathrm{pHs} = (9.3 + \mathrm{A} + \mathrm{B}) - (\mathrm{C} + \mathrm{D})$$

$$\mathrm{A} = \mathrm{Log10}\left(\text{salinity in mg. L}^{-1}\right) - 1/10$$

$$\mathrm{B} = -13.12 \times \mathrm{Log10}\,(\text{temperature in }^{\circ}\mathrm{C} + 273) + 34.55$$

$$\mathrm{C} = \mathrm{Log10}\left(\text{calcium hardness in mg. L}^{-1}\right) - 0.4$$

$$\mathrm{D} = \mathrm{Log10}\left(\text{TAC in mg. L}^{-1}\right)$$

An RSI below 7 indicates scaling water that will lead to calcium carbonate deposits if left untreated. Conversely, an RSI above 7 signifies aggressive and corrosive water.

When applied to the Ras Elma spring water, the RSI fluctuates between 6.6 and 8, indicating that the majority of Ras Elma's water is aggressive. However, during July, August, and September, the water's nature changes to deposit calcium carbonate. Meanwhile, Oued El Heddar's water shows a value above 7 throughout the measured months, signifying aggressiveness, except for month 9, which records a value of 6.8 (Fig. 8).

Langelier's method is a commonly employed approach in physico-chemical studies to assess water aggressiveness. The calculation follows this equation:

$$\mathrm{LSI} = \mathrm{pH} - \mathrm{pHs}$$

where: pH represents the measured pH of the solution,

pHs signifies the saturation pH concerning calcite, calculated as follows:

$$\mathrm{pHs} = \mathrm{pk'2} - \mathrm{pk's} - \log\left(\mathrm{Ca}^{2+}\right) - \log\,(\mathrm{TA}) - \log(1 + 2.10(\mathrm{pHs} - \mathrm{pk's}))$$

Langelier utilizes equilibrium constants pk'2 and pk's, denoting the apparent constants of the 2nd dissociation of carbonic acid and the solubility product of calcite, respectively. For pH values below 9.5, Langelier suggests disregarding the term log(1 + 2.10(pHs-pk's)).

This leads to the simplified formula: $\mathrm{pHs} = \mathrm{pk'2} - \mathrm{pk's} - \log\,(\mathrm{Ca}^{2+}) - \log\,(\mathrm{TA})$.

According to Langelier:

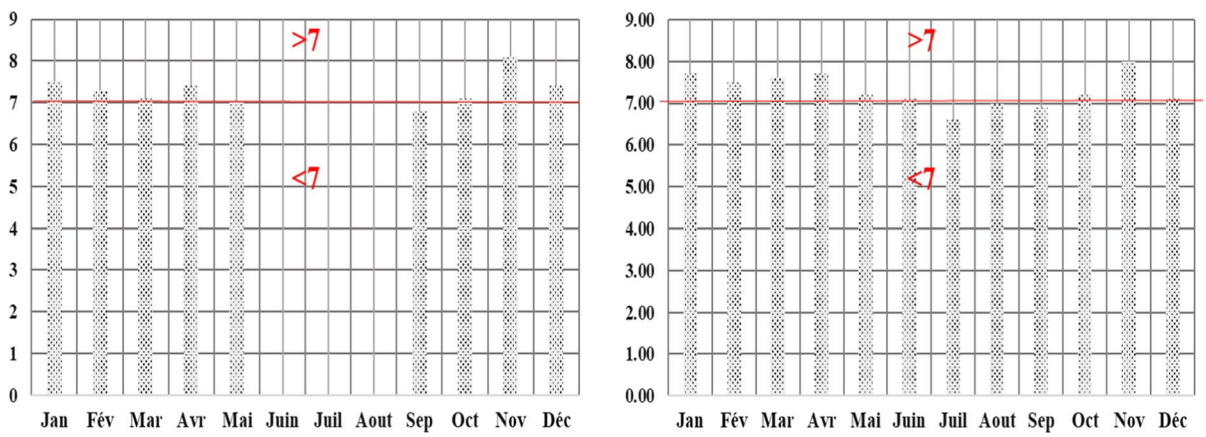

Fig. 8 The nature of the water in Ras Elma and Oued El Heddar according to the Ryznar Index (RI)

- LSI < 0 implies that the water's measured pH is lower than the saturation pHs, indicating undersaturation in calcite.
- LSI = 0 denotes equality between the measured water pH and saturation pHs, indicating saturation and calco-carbonic equilibrium.
- LSI > 0 suggests that the water's measured pH exceeds the saturation pHs, signifying supersaturation in calcite, leading to $CaCO_3$ precipitation.

According to this index (Fig. 9), it appears that the majority of water from the Ras Elma source is undersaturated in calcite, except for the months of July, August, September, and December, which are saturated in calcite and tend to precipitate $CaCO_3$. However, the water of Oued El Heddar is saturated in calcite throughout the measurement year of 2021, except for the month of November.

This index suggests minimal dissolution of carbonate rocks in the Dayat Chikker aquifer. The dissolution of calcite consumes carbon dioxide (Al-Droubi, 1976) and affects the pH level. Conversely, at the level of Oued El Heddar, it appears that the water flowing from the Ras Elma source until it meets Oued Benoune consumes more carbon dioxide from the air. This makes the water more aggressive towards carbonate rocks, resulting in the supersaturation of calcium carbonate in Oued El Heddar.

Moreover, in predicting the theoretical rate of precipitated calcium carbonate during the measurement year, we referenced the work of Hallopeau–Dubin, 1960. This work relies on physico-chemical parameters such as water temperature, pH, TAC (Total Alkalimetric Title), calcium, dry residue, chloride, and sulphates.

According to this index (Fig. 10), it appears that calcium carbonate $CaCO_3$ precipitation at the Ras Elma spring occurs in July, August, September, October, and December, with rates varying between 12mg/l in October and 42mg/l in July. However, $CaCO_3$ is soluble in January, March, April, and November, while February, May, and June are characterized by the absence of $CaCO_3$. Conversely, at the downstream point, Oued El Heddar, there is $CaCO_3$ precipitation during the measurement months, except for June, July, and August, when Oued El Heddar is dry.

This differentiation between the upstream spring water and downstream Oued El Heddar can be explained by numerous factors such as precipitation rates, temperature, and the level of free carbon dioxide (CO_2). The latter factor holds a greater influence on the potential for calcium carbonate precipitation.

Discussion

In light of these results, and though we were limited to a single day of hydrochemical analysis per month at the three sites, it's evident that the Ras Elma spring water was undersaturated in calcium carbonate during November, January, March, and April of the 2021 measurement year. Conversely, the water was

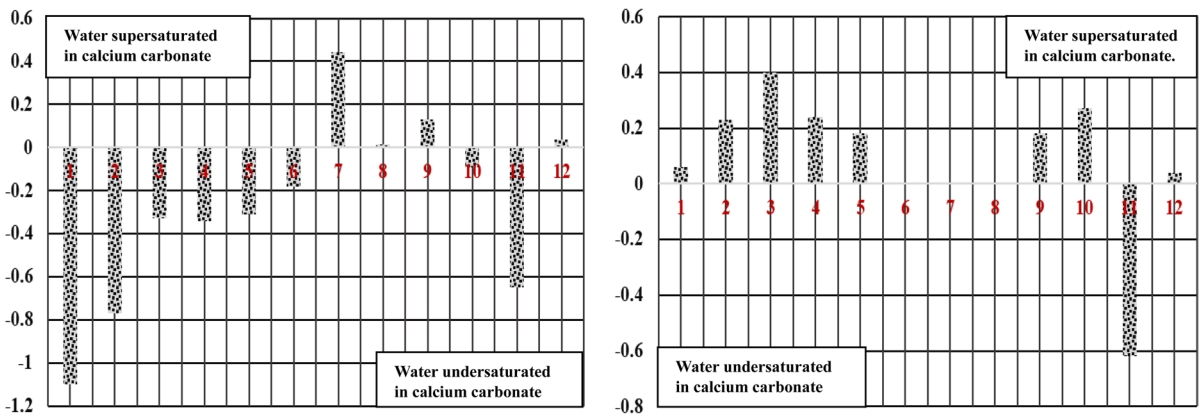

Fig. 9 LSI of Ras Elma and Oued El Heddar

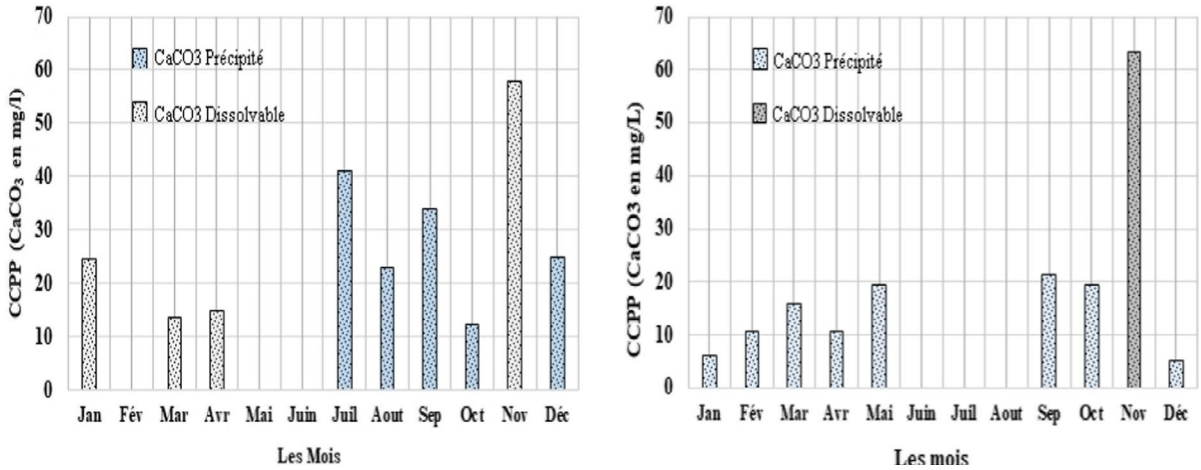

Fig. 10 Potential for precipitation of calcium carbonate (PPCC) in Ras Elma and Oued Heddar

supersaturated in $CaCO_3$ during July, August, and September (a period when Morocco faced a drought and significant water deficit from 2019 to 2023). This new scenario disrupts and influences the system of calcite dissolution and precipitation within the Chikker cave's endokarst, leading to an imbalance in the travertinisation system in the Ras Elma region.

Carbon dioxide dissolved in water plays a vital role in limestone dissolution (Mitchell et al., 2010; Mark et al., 2010), although not the sole factor, yet generally the most significant (Ek, 1973). Additionally, water from Ras Elma's Chikker endokarst, likely rich in CO_2 as indicated by the research in Belgium by (EK & Gewelt, 1985), confirms that CO_2 levels in cave air are notably higher than those in open air. While open-air concentrations are around 400ppm, cave levels vary from 1000 to 30000ppm, at times even higher. According to Henry's law, the CO_2 content in water maintains equilibrium with that of the ambient air (Atkinson, 1977).

In Taza, only Wassenburg's work in 2013 on the Piste Grotto, located about 30km west of Taza at coordinates 341N; 041W, indicated variations in temperature between 11.8°C in winter and 13.3°C in summer, with an average annual Pco_2 rate of 666 ± 151, a rate affected by ventilation fluctuations inside the cave, as per the same researcher. However, there's no precise measurement work to date on the Pco_2 within the Chikker cave. We anticipate that the Pco_2 rate will progressively increase inside the cave, possibly being higher than the Piste cave due to several factors, notably the limited orifices only the two adjoining ones connected near Dayat Chikker. This leads us to predict a progressively higher Pco_2 rate inside the cave, particularly in summer.

The dissolution of calcium carbonate during the summer season can be attributed to several factors, including temperature disparities between the cave and open air (colder air inside the cave in summer and the opposite in winter) and increased Pco2 during summer compared to winter (Gewelt & Ek, 1986), which intensifies rock dissolution within the caves. Consequently, it likely leads to the probable precipitation of $CaCO_3$ and the formation of travertines in summer within the Ras Elma region (Campbell et al., 2017).

The lower section of the Ras Elma spring, exhibiting various tuff and travertine formations, is observable from the ground, particularly where the flow is concentrated, with a substantial variation in depth of up to 1m in the already formed travertines (Fig. 11).

Hollowing out ras elma spring water in the travertines

After understanding the state and hydrochemical nature of Ras Elma's spring water, it becomes evident that from the large café in Ras Elma to the grand cascade, we find a succession of several well-preserved travertine dams in certain locations. Conversely, the

Fig. 11 Digging Ras Elma spring water into the travertine

increased water concentration in the main channel of Oued El Heddar has reversed the situation in which the dam was constructed. In other words, while the water from the dams was previously instrumental in constructing the travertine dams, its intensified concentrations now, induced by the hydrochemical nature of the water and unfavorable climatic changes, are dismantling what had been built.

The slight increase in the $CaCO_3$ precipitation level in the Oued El Heddar valley during early spring can be attributed to various factors. Water agitation based on the current morphology of the Oued El Heddar channel and the influence of aquatic flora (mosses, algae, roots) along the channel edges, as well as bacterial activity, especially during the vegetative season (spring–summer), are elements contributing to this increase (Adolphe, 1981; Casanova, 1981; Muxart, 1981). However, it is crucial to note that during the months of June, July, and August, the Oued El Heddar experienced periods of drought due to minimal or nonexistent water flow at the sampling point, attributed to significant human interference upstream, near the center of Ras Elma. The diversion of water from the Oued El Heddar channel for agricultural irrigation on small terraces significantly contributes to the degradation of travertine formation in the region. These factors underscore the importance of human activity and local ecology in the travertine formation process, as well as the potential impact of water resource management on the geological and hydrochemical environment of the region.

Conclusion

The impact of water chemistry on the formation of present-day travertines in the Ras Elma region is a complex and intricate process. This study has enabled us, on the one hand, to highlight the main geochemical mechanisms that compose the Ras Elma spring water resulting from the infiltration of the Dayat Chikker endokarst. Secondly, it aimed to determine the water's nature based on the calcaro-carbonic methods of Ryznar, Langelier, and Hallopeau to ascertain the state of travertinisation in the study area,

confirmed by field verification. This work led to the following results:

- The geological context and spatial distribution of the chemical elements indicate that the dominant facies are the calcic bicarbonate facies, with the chemical composition of the groundwater in the Ras Elma aquifer strongly influenced by the dissolution of the Liasic and argilo-triasic carbonate formations and by the hydrological parameters of the region, such as the flow direction and residence time in the Ras Elma-Laansseur aquifer.
- According to Ryznar's index, Ras Elma spring water is aggressive during July, August, and September, leading to calcium carbonate deposition. Langelier's index indicates that most of Ras Elma spring water is undersaturated with calcite, except in July, August, September, and December, which are saturated with calcite and tend to precipitate $CaCO_3$. Moreover, Oued El Heddar's water is saturated with calcite during the 2021 measurement year, except for November.
- Furthermore, according to the CCPP index, precipitation of calcium carbonate $CaCO_3$ at the Ras Elma source occurs from July to December, with rates varying between 12 mg/l in October and 42 mg/l in July. Conversely, the downstream point, Oued El Heddar, experiences precipitation of $CaCO_3$ throughout the measurement months, except in June, July, and August when Oued El Heddar was dry.
- Physico-chemical precipitation is currently undergoing a pronounced inhibition and decline in the spring waters of Ras Elma, marked by the excavation and destruction of ancient travertines previously formed. However, travertinisation remains active, mainly due to the agitation of chemical reactions, particularly at dams and waterfalls. Valley travertines, on the other hand, are more developed due to water agitation, the role of aquatic vegetation (mosses, algae, etc.), and increased solution temperature.
- In addition to the geochemical role of water, other factors contribute to the decline of travertine in the center of Ras Elma, such as the alteration of water chemistry, often due to decreased CO2 flow either because of climate change or anthropogenic impact. The decline of travertine in the region is also attributed to pollution, which sometimes inhibits the development or action of carbonatogenic micro-organisms.

Author contributions KL, ML, and JG collaborated on the overall design of the study, the development of the methodology, and the field data collection. KL and AO conducted all physico-chemical analyses of the recovered waters. JN and JG contributed to data analysis, particularly concerning geochemical aspects, while HF participated in map creation. The initial draft of the manuscript was written by KL and ML, with all authors contributing to its refinement. All authors have reviewed the final manuscript and approved it.

Funding The study did not receive any external funding.

Availability of data and material All data generated during the manuscript analysis are included in the article. Further datasets are available from the corresponding author upon request.

Declarations

Conflict of interest The authors declare that they have no competing interests.

References

Adolphe, J. (1981). Exemples de contribution microorganiques dans les constructions carbonatées continentales. In *Actes du colloque de l'AGF, formations carbonatées externes*. Tufs et travertins, Paris.

Akin, M., & Özsan, A. (2011). Evaluation of the long-term durability of yellow travertine using accelerated weathering tests. *Bulletin of Engineering Geology and the Environment, 70*(1), 101–114. https://doi.org/10.1007/s10064-010-0287-x

Al-Droubi, A. (1976). Géochimie des eaux et des sels dans les sols des polders du lac Tchad : Application d'un modèle thermodynamique de simulation de l'évaporation. *Chemical Geology, 17*, 165–177.

Al-Qurnawi, W. S., Ghalib, H. B., Alabadi, M. A. A., & Al-Hawash, A. B. (2022). Corrosion: Scaling potentially of domestic water pipelines and evaluate the applicability of raw water sources in Basrah IRAQ. *Iraqi Journal of Science, 63*(5), 2089–2102. https://doi.org/10.24996/ijs.2022.63.5.24

Amouei, A. I., Yousefi, Z., & Khosravi, T. (2017). Comparison of vermicompost characteristics produced from sewage sludge of wood and paper industry and household solid wastes. *Journal of Environmental Health Science & Engineering, 15*, 5. https://doi.org/10.1186/s40201-017-0269-z

Andrews, J. E. (2006). Paleoclimatic records from stable isotopes in riverine tufas: Synthesis and review. *Earth-Science Reviews, 75*(1), 85–104. https://doi.org/10.1016/j.earscirev.2005.08.002

Asta, M. P., Auqué, L. F., Sanz, F. J., Gemeno, M. J., Acero, P., Blasco, M., Garcia-Alix, A., & Atkinson, T. C. (1977).

Carbon dioxide in the atmosphere of the unsaturated zone: an important control of groundwater hardness in limestones. *Journal of Hydrology, 35*(1–2), 111–123. https://doi.org/10.1016/0022-1694(77)90080-4

Bakalowicz, M. (1990). Géochimie des eaux incrustantes, formation des travertins et néotectonique: l'exemple des Corbières. Travaux du groupe Seine Bulletin Centre Géomorphologie.

Bonny, S. M., & Jones, B. (2008). Controls on the precipitation of barite ($BaSO_4$) crystals in calcite travertine at Twitya Spring, a warm sulphur spring in Canada's Northwest Territories. *Sedimentary Geology, 203*(1), 36–53. https://doi.org/10.1016/j.sedgeo.2007.10.003

Campbell, J., Fletcher, W., Joannin, S., Hughes, P. J., Rhanem, M., & Zielhofer, C. (2017). Environmental drivers of holocene forest development in the Middle Atlas. *Morocco. Frontiers in Ecology and Evolution*. https://doi.org/10.3389/fevo.2017.00113ff

Casanova, J. (1981). Morphologie et biolithogenèse des barrages de travertin, formations carbonatées externes, tufs et travertins, Edition du Comité national de Géographie Française, in *Mémoire de l'Association Française de Karstologie*, n°3

Chafetz, H. S., & Folk, R. L. (1984). Travertines: Depositional morphology and the bacterially constructed constituents. *Journal of Sedimentary Petrology, 54*(1), 289–316. https://doi.org/10.1306/212F8404-2B24-11D7-8648000102C1865D

Claes, H., Erthal, M. M., Soete, J., Ozkul, M., & Swennen, R. (2017). Shrub and pore type classification: Petrography of travertine shrubs from the Ballık-Belevi area (Denizli, SW Turkey). *Quaternary International, 437*, 147–163. https://doi.org/10.1016/j.quaint.2016.11.002

Cook, M., & Chafetz, H. S. (2017). Sloping fan travertine, Belen, New Mexico USA. *Sedimentary Geology, 352*, 30–44. https://doi.org/10.1016/j.sedgeo.2017.02.010

Drysdale, R., Taylor, M., & Ihlenfeld, C. (2002). Factors controlling the chemical evolution of travertine-depositing rivers of the Barkely karst, north Australia. *Hydrological Processes, 16*, 2941–2962. https://doi.org/10.1002/hyp.1078

Ehya, F., & Marbouti, Z. (2018). Groundwater quality assessment and its suitability for agricultural purposes in the Behbahan Plain, SW Iran. *Water Practice & Technology, 13*(1), 62–78. https://doi.org/10.2166/wpt.2018.001

EK, C. (1973). Analyses d'eaux des calcaires paléozoiques de la Belgique. Méthodes – techniques – résultats. *Geological Survey of Belgium, 1973/18* - 101.

Ek, C., & Gewelt, M. (1985). Carbon dioxide in cave atmospheres. New results in Belgium and comparison with some other countries. *Earth Surface Processes and Landforms, 10*(2), 173–187.

Ford, T. D., & Pedley, H. M. (1996). A review of tufa and travertine deposits of the world. *Earth-Science Reviews, 41*(3–4), 117–175. https://doi.org/10.1016/S0012-8252(96)00030-X

Foucault, A. & Raoult, F. (1980). Dictionnaire de Géologie. Dunod, 1° Edition.

Fouke, B. W., Farmer, J. D., Des Marais, D. J., Pratt, L., Sturchio, N. C., Burns, P. C., & Discipulo, M. K. (2000). Depositional facies and aqueoussolid geochemistry of travertine-depositing hot springs (Angel Terrace, Mammoth Hot Springs, Yellowstone National Park, U.S.A.). *Journal of Sedimentary Research, 70*(3), 565–585. https://doi.org/10.1306/2dc40929-0e47-11d7-8643000102c1865d

Gentil, L. (1911) Les grandes lignes du relief marocain. *Revue générale des Sciences*, 22e année, p. 486–493.

Gewelt, M. & Ek, C. (1986). L'évolution saisonnière de la teneur en CO2 de l'air de deux grottes belges: Ste-Anne et Brialmont, Tilff. In K. Paterson & M.M. Sweeting (Eds.) *New directions in Karst* (pp. 49–76).

Ghobadi Nia, M., Rahimi, H., Sohrabi, T., Naseri, A., & Tofighi, H. (2010). Potential risk of calcium carbonate precipitation in agricultural drain envelopes in arid and semi-arid areas. *Agricultural Water Management., 97*(10), 1602–1608. https://doi.org/10.1016/j.agwat.2010.05.014

Hallopeau, J. (1960). Les équilibres carboniques dans les eaux. *Terres Et Eaux, 35*(2), 4.

Hoepffner, C. (1978). Le massif paléozoïque de tazekka (Maroc); analyse des déformations liées à un linéament tectonique. *Sciences Géologiques, Bulletins Et Mémoires, 31*(1), 33–44.

Ismail, S., & Ahmed, M. F. (2023). Hydrogeochemical characterization of the groundwater of Lahore region using supervised machine learning technique. *Environmental Monitoring and Assessment, 195*(1), 1–26. https://doi.org/10.1007/s10661-022-10648-x

ISO (1994) Systèmes qualité - Modèle pour l'assurance de la qualité en conception, développement, production, installation et prestations associées.

Kalender, L., Ozlem, O. O., Murat, I., Bahattin, C., & Vesile, Y. (2015). Geochemistry of travertine deposits in the Eastern Anatolia District: An example of the Karakoçan-Yoğunağaç (Elazığ) and Mazgirt-Dedebağ (Tunceli) travertines, Turkey. *Turkish Journal of Earth Sciences, 24*(6), 607–626. https://doi.org/10.3906/yer-1504-27

Kele, S., Demény, A., Siklósy, Z., Nemeth, T., Toth, M., & Kovacs, M. B. (2008). Chemical and stable isotope composition of recent hot-water travertines and associated thermal waters, from Egerszalók, Hungary: depositional facies and non-equilibrium fractionation. *Sedimentary Geology, 211*(3), 53–72. https://doi.org/10.1016/j.sedgeo.2008.08.004

Liu, Y. P., Zhou, X., Deng, Z. J., Fang, B., TsutomuY, Z. J. B., & Wang, X. C. (2015). Hydrochemical characteristics and genesis analysis of the Jifei hot spring in Yunnan, southwestern China. *Geothermics, 53*, 38–45. https://doi.org/10.1016/j.geothermics.2014.04.002

Luo, L., Wen, H., Brogi, A., & Capezzuoli, E. (2022). Factors controlling the geometry of travertine mounds: Insights from Heinitang (China). *Sedimentology, 69*(4), 1519–1546. https://doi.org/10.1111/sed.12961

Mitchell, M. J., Jensen, O. E., Cliffe, K. A., & Maroto-Valer, M. M. (2010). A model of carbon dioxide dissolution and mineral carbonation kinetics. *Proc. r. Soc. A, 466*, 1265–1290. https://doi.org/10.1098/rspa.2009.0349

Mounir, S., Saoud, M., Charroud, K., Mounir, J., & Choukrad, J. (2019). The Middle Atlas Geological karsts forms: Towards Geosites characterization. *Oil & Gas Science and Technology - Rev. IFP Energies Nouvelles 74*, 17. https://doi.org/10.2516/ogst/2018089

Muxart, T. (1981) Thème II. Processus de précipitation et mesures (Process of precipitation and measures) Bulletin de l'Association de Géographes Français, 479–480 (pp. 189–196).

Nicod, J. (1986). Facteurs physico-chimiques de l'accumulation des formations travertineuses, revue géographique des pays méditerranéen (pp. 161–164).

Özkul, M., Kele, S., Gökgöz, A., Shen, C. C., Jones, B., Baykara, M. O., Fórizs, I., Nemeth, T., Chang, Y. W., & Alcicek, M. C. (2013). Comparison of the quaternary travertine sites in the Denizli extensional Basin based on their depositional and geochemical data. *Sedimentary Geology, 294*(3), 179–204. https://doi.org/10.1016/j.sedgeo.2013.05.018

Palazzo, A., van der Merwe, J., & Combrink, G. A. (2015). The accuracy of calcium-carbonate based saturation indices in predicting the corrosivity of hot brackish water towards mild steel. *Journal of the Southern African Institute of Mining and Metallurgy., 115*(12), 1229–1238. https://doi.org/10.17159/2411-9717/2015/v115n12a12

Pentecost, A. (1995). Geochemistry of carbon dioxide in six travertine-depositing waters of Italy. *Journal of Hydrology, 167*(1–4), 263–278. https://doi.org/10.1016/0022-1694(94)02596-4

Pentecost, A. (2005). *Travertines*. Springer.

Plummer, L.N. (1984). Geochemical modeling: A comparison of forward and inverse methods. In: Hitchon, B. & Wallick, E.I. (eds.) *Practical Applications of Ground Water Geochemistry. First Canadian/American Conf Hydrogeol* (pp. 149–177).

Quade, J., Rasbury, E. T., Huntington, K. W., Hudson, A. M., Vonhof, H., Anchukaitis, K., Betancourt, J., Latorre, C., & Pepper, M. (2017). Isotopic characterization of late Neogene travertine deposits at Barrancas Blancas in the eastern Atacama Desert, Chile. *Chemical Geology, 466*, 41–56. https://doi.org/10.1016/j.chemgeo.2017.05.004

Rimstidt, D. J., & Vaughan, J. D. (2003). Pyrite oxidation: a state-of-the-art assessment of the reaction mechanism. *Geochimica Et Cosmochimica Acta., 67*(5), 873–880. https://doi.org/10.1016/S0016-7037(02)01165-1

Robillard, D. (1981). Etude stratigraphique et structurale du Moyen Atlas Septentrional (Région de Taza-Maroc). Thèse 3° cycle, Lille.

Rodier, J., Legube, B., Merlet, N., & Brunet, R. (2009). L'analyse de l'eau. Eauxnaturelles, eaux résiduaires, eaux de mer, 9ème édition–pris: dumod. 1579.

Sabaoui, A., & Viallard, P. (1987). Fractures majeures et décollement de couverture dans le moyen atlas septentrional (sud-ouest de Taza, Maroc). In C.R Acad. Sc., 305, série 2, Paris.

Santhanam, H., Karthikeyan, A., & Raja, M. (2021). Saturation indices of aqueous mineral phases as proxies of seasonal dynamics of a transitional water ecosystem using a geochemical modeling approach. *Modeling Earth Systems and Environment., 7*, 1813–1829. https://doi.org/10.1007/s40808-020-00910-x

Srour, E., Hussien, R. A., & Moustafa, W. M. (2022). Geochemical modeling and isotopic approach for delineating water resources evolution in El Fayoum depression, Egypt. *Environmental Earth Sciences, 81*, 105. https://doi.org/10.1007/s12665-022-10192-4

Teboul, P. A., Durlet, C., Gaucher, E. C., Virgone, A., Girard, J. P., Curie, J., Lopez, B., & Camoin, G. F. (2016). Origins of elements building travertine and tufa: New perspectives provided by isotopic and geochemical tracers. *Sedimentary Geology, 334*, 97–114. https://doi.org/10.1016/j.sedgeo.2016.01.004

Thiry, M. & Jean, G. (2013). Les tufs quaternaires de La Celle-sur-Seine (77). En commémoration de la première sortie géologique de l'ANVL, le 12 février 1922. ffhal-00857687f. https://minesparis-psl.hal.science/hal-00857687

Vaudour, J. (1986). Travertins holocènes et pression anthropique. *Méditerranée, 1–2*, 168–172. https://doi.org/10.3406/medit.1986.2389

Wassenburg, J. A., Immenhauser, A., Richter, D. K., Niedermayr, A., Riechelmann, S., Fietzke, J., Scholz, D., Jochum, K. P., Fohlmeister, J., Schröder-Ritzrau, A., Sabaoui, A., Riechelmann, D. F. C., Schneider, L., & Esper, J. (2013). Moroccan speleothem and tree ring records suggest a variable positive state of the North Atlantic Oscillation during the Medieval Warm Period. *Earth, and Planetary Science Letters, 375*(2013), 291–302. https://doi.org/10.1016/j.epsl.2013.05.048

Weisrock, A., Delibrias, G., Miskovsky, J.C., Dutour, A., & Adolphe, J.P. (1986). Un exemple de sédimentation carbonatée holocène de type travertineux sur le piémont nord du haut atlas (Maroc) : la coupe de makhfamane I. Méditerranée, 1–2, Actes de la Table-Ronde sur « travertins l.s et évolution des paysages holocènes dans le domaine méditerranéen » Aix-en-povence, 1985, pp. 39–44

Yan, F., Dong, F., & Yang, G. (2023). Travertine and mid-ocean ridges are related analogues regarding geographical location and sedimentary model. *Polish Journal of Environmental Studies, 32*(1), 399–404. https://doi.org/10.15244/pjoes/153927

Yekta, R.M., Kaykhah, H., Dilkhah, M. & Nohani, E. (2015). Evaluation of the quality of water treatment plant sewage for reuse in agriculture in ilam. *Applied Research Journal* 1(5). ISSN: 2423–4796

Zhang, J., Wang, H., Liu, Z., An, D., & Dreybrodt, W. (2012). Spatial–temporal variations of travertine deposition rates and their controlling factors in Huanglong Ravine, China – a world's heritage site. *Applied Geochemistry, 27*(1), 211–222. https://doi.org/10.1016/j.apgeochem.2011.10.005

Zhao, D., Zeng, Y., Wu, Q., Mei, A., Gao, S., Du, X., & Yang, W. (2022). Hydrogeochemical characterization and suitability assessment of groundwater in a typical coal mining subsidence area in China using self-organizing feature map. *Environment and Earth Science, 81*(21), 1–17. https://doi.org/10.1007/s12665-022-10596-2